

VREM-FL: Mobility-Aware Computation-Scheduling Co-Design for Vehicular Federated Learning

Luca Ballotta[✉], *Member, IEEE*, Nicolò Dal Fabbro[✉], *Graduate Student Member, IEEE*,
Giovanni Perin[✉], *Member, IEEE*, Luca Schenato[✉], *Fellow, IEEE*, Michele Rossi[✉], *Senior Member, IEEE*,
and Giuseppe Piro[✉], *Member, IEEE*

Abstract—Assisted and autonomous driving are rapidly gaining momentum, and will soon become a reality. Among their key enablers, artificial intelligence and machine learning are expected to play a prominent role, also thanks to the massive amount of data that smart vehicles will collect from their onboard sensors. In this domain, federated learning is one of the most effective and promising techniques for training global machine learning models, while preserving data privacy at the vehicles and optimizing communications resource usage. In this work, we propose VREM-FL, a computation-scheduling co-design for vehicular federated learning that leverages mobility of vehicles in conjunction with estimated 5G radio environment maps. VREM-FL jointly optimizes the global model learned at the server while wisely allocating communication resources. This is achieved by orchestrating local computations at the vehicles in conjunction with the transmission of their local model updates in an adaptive and predictive fashion, by exploiting radio channel maps. The proposed algorithm can be tuned to trade model training time for radio resource usage.

Experimental results demonstrate the efficacy of utilizing radio maps. VREM-FL outperforms literature benchmarks for both a linear regression model (learning time reduced by 28%) and a deep neural network for a semantic image segmentation task (doubling the number of model updates within the same time window).

Index Terms—5G, Federated Learning, optimization, REM, resource management, scheduling, vehicular networks.

I. INTRODUCTION

AMONG the most popular verticals of fifth generation (5G) and beyond communications, connected cars has the highest annual growth rate according to Cisco [1]. In 2021, Siemens estimated that the amount of data generated by autonomous vehicles will range from 3 to 40 Gbit/s depending on the autonomy level [2], which amounts to up to 19 TB every hour.

This work was supported in part by the Italian Ministry of Education, University and Research (MIUR) through the PRIN Project under Grant 2017NS9FEY entitled “Realtime Control of 5G Wireless Networks” and by the European Union under the Italian National Recovery and Resilience Plan (NRRP) of NextGenerationEU, partnership on “Telecommunications of the Future” (PE0000001 – program “RESTART”). (Luca Ballotta, Nicolò Dal Fabbro, and Giovanni Perin contributed equally to this work).

Luca Ballotta, Nicolò Dal Fabbro, Giovanni Perin, Luca Schenato, and Michele Rossi are with the Department of Information Engineering, University of Padova, 35131 Padova, Italy (e-mail: {luca.ballotta; giovanni.perin.l; l.schenato; michele.rossi}@unipd.it, nicolo.dalfabbro@phd.unipd.it).

Michele Rossi is also with the Department of Mathematics “Tullio Levi-Civita,” University of Padova, 35121 Padova, Italy.

Giuseppe Piro is with the Department of Electrical and Information Engineering, Politecnico di Bari, 70125 Bari, Italy, and with the Consorzio Nazionale Interuniversitario per le Telecomunicazioni, 43124 Pisa, Italy (e-mail: giuseppe.piro@poliba.it).

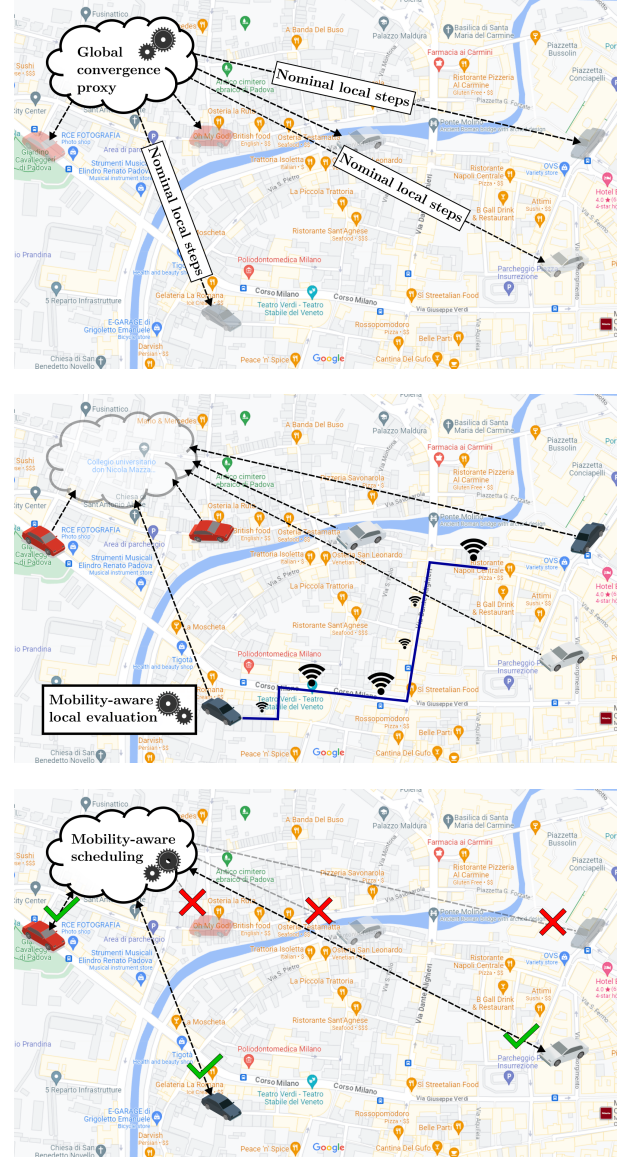


Fig. 1. VREM-FL. The mobility-aware co-design proposed in this article.

The huge availability of data in modern vehicular networks paves the way to training, possibly at runtime, large deep learning models. Nowadays, this is mostly accomplished via *federated learning* (FL), which is the most prominent solution from the state-of-the-art to train neural networks from the data collected by distributed clients. FL has several advantages, such as high flexibility, offered by the possibility of choosing when

local models are to be sent by the end users to the central aggregator, and offers a certain degree of privacy, due to the fact that end-user data is never transmitted: only the model weights are sent from the end-users to the aggregator.

Remarkably, despite the extensive amount of work available on communication-constrained [3], [4] and channel-aware [5], [6] FL algorithms, scheduling policies for vehicular networks that jointly consider mobility, communication/channel resources, and learning aspects are currently lacking.

In the present article, these aspects are *jointly* tackled for the first time, proposing vehicular radio environment map (REM) federated learning (VREM-FL), an FL scheduler that orchestrates the computation and the transmission of local models from the end users (the vehicles) to the central model aggregator (at the roadside network). VREM-FL exploits the availability of REMs to pick the most profitable transmission instants for the transmission of the local models from the vehicles. This is possible due to the fact that REMs are relatively stable over time [7], [8], as they mainly depend on static obstacles, such as buildings in urban environments. Hence, their knowledge can be combined with information on the planned user routes to attain optimal FL transmission schedules. The optimization criteria correspond to minimizing the channel resources that are wasted due to transmitting when the channel conditions are poor, and to meeting a deadline for the global model update.

VREM-FL organizes the learning task into three stages, see Fig. 1 from top to bottom: (1) the central orchestrator, based on channel and computation resources, decides how many vehicles are allowed to participate in the current round, proposes an initial number of iterations for the update of their local models, and sets a maximal round latency (deadline); (2) all the vehicles, based on their private planned routes, learning metrics, and available REMs, adjust the number of local iterations received by the orchestrator, and decide when to transmit their own models; (3) the orchestrator, upon receiving the vehicles' feedback, chooses the best subset of them to take part in the current round. The selected vehicles update their local models and send their model updates to the orchestrator. The received updates are finally used at the orchestrator to refine the global model.

Novel contributions: The main contributions of this article are summarized as follows.

- We propose VREM-FL, a computation-scheduling co-design tailored to vehicular FL. VREM-FL leverages the knowledge of vehicles' routes and REMs, to optimize the communication resources used by the vehicles, while also ensuring high learning performance.
- A realistic simulation environment is implemented in Python using the street map of the city of Padova (Italy) and the popular simulator of urban environment (SUMO) [9]. On this map, base stations (BSs) are deployed according to typical parameters of 5G cellular systems [10], to provide communications services to the vehicles. To capture realistic settings, where channel quality measurements are only available in a limited number of geographical locations, REMs are obtained via Gaussian process regression [8], [11].

- VREM-FL is evaluated via an extensive simulation campaign comprising (i) controlled experiments with a least squares (LS) toy example and (ii) a more realistic scenario involving the execution of a semantic segmentation task on the popular ApolloScape [12] dataset. Moreover, VREM-FL is compared with literature benchmarks such as vanilla *federated averaging* (FedAvg) [13] (*i.e.*, random selection of clients) and the algorithm in [14], where a fairness metric for the selection of the vehicles is considered.

The rest of this paper is organized as follows. In Section II the state-of-the-art is presented; Section III provides a general overview of VREM-FL. In Section IV, the system model is presented, including the FL setup and the radio environment settings. The problem is defined in Section V, while VREM-FL is detailed in Section VI. Numerical simulation results demonstrating the effectiveness of VREM-FL are presented in Section VII. Finally, conclusions are drawn in Section VIII, along with future research directions.

II. RELATED WORK

In this section, the state-of-the-art on FL over wireless networks is reviewed, focusing on the previous efforts on computation-communication co-design methods and on the existing solutions for vehicular FL. Some relevant approaches to leverage REMs for wireless resource management are also discussed, underlining the novelty of our solution.

A. User Scheduling for FL in Wireless Networks

Lately, many research works have investigated scheduling techniques for FL over wireless networks [15], [16], [17], [18], [19]. In [20], scheduling policies were experimented with by simulating users connected to different access points together with different signal-to-interference-plus-noise ratio (SINR) thresholds. The recent work [21] proposed PALORA, a scheduling method jointly considering fairness with respect to the local models, signal-to-noise ratio (SNR) levels, and resource blocks utilization. Along the same lines, the paper [14] considered asynchronous updates, took into account the computation-communication tradeoff, and proposed scheduling strategies based on *age-of-information* (AoI) and *fairness*. This paper presented experiments with realistic FL training time estimates over wireless networks. In [22], scheduling was performed based on data quality metrics establishing a user priority indicator, which is used to jointly solve a user selection and bandwidth allocation problem. A scheduling approach based on data selection was proposed in [23], where the gradient norm was used to compute a metric that relates learning efficiency with data selected by users for local training. The authors of [24] proposed a scheduling policy for FL over an orthogonal frequency-division multiple access (OFDMA) scheme where scheduling decisions are based on learning accuracy and channel quality.

B. FL in Vehicular Networks

There is a growing interest in machine learning solutions for problems related to vehicular networks, given the increasing need for data-driven algorithms in intelligent transportation

systems [25]. Applications examples include wireless resource management [26], traffic flow prediction [27], vehicle-based perception for autonomous driving [28], [29], to name a few.

With respect to the federated training setup, some works have focused on *static* vehicular federated learning [30], [31], with particular emphasis on scenarios involving parking lots [32] and related issues, like parking space estimation.

Conversely, cooperative training of machine learning models in scenarios involving user mobility, as in vehicular networks, is still an open and key research objective [33], [34]. In this context, several works have recently considered vehicular FL for, e.g., image classification problems [35], proactive caching [36], and object detection [37].

Recently, other works have investigated the allocation and optimization of network resources in vehicular FL [38], [39], [40], [41], [42]. Specifically, the work [40] analyzed the impact of vehicular mobility on wireless transmissions, proposing wireless network optimization techniques to improve the performance. The authors of [42] considered cache queue optimization at the edge server, while other related scheduling techniques were proposed in [38], [39]. On the other hand, the authors of [41] focused on tuning the number of local iterations based on mobility awareness in relation to short-lived connections with the base stations. The work [43] studied the adoption of FL in an IoV scenario where vehicles communicate with 5G base stations, exploiting context information such as cell association and mobility prediction together with the related channel quality for users' scheduling.

However, none of the above-mentioned works leverages the combination of *mobility patterns* and *radio environmental awareness* to optimize the learning performance of federated learning while at the same time optimizing wireless network resources. Our work is the first to jointly consider these aspects which, as we shall see, leads to sizeable advantages over previous solutions.

C. REMs for Wireless Resource Management

A radio environment map (REM) is a geographic database of average communication quality metrics. In recent years, REMs have been proposed as an effective tool to manage wireless resources [7]. For example, REMs have been advocated for predictive resource allocation [44] and handover management in 5G networks [45]. Recently, in 5G systems with massive multiple-input multiple-output (mMIMO) transmission, REMs have been adopted for energy efficient design [46], inter-cell interference coordination [47], beam management [48], and cell-edge users throughput improvement via dynamic point blanking [49]. Even though the use of REMs has been investigated for several resource management applications in wireless communications, this work is the first to exploit them for network resources optimization in FL and, specifically, in vehicular FL.

III. VREM-FL IN A NUTSHELL

In this article, we are concerned with optimal resource allocation for FL tasks executed by vehicles traveling within an urban environment and an edge server acting as a centralized aggregator of the model. In what follows, we interchangeably

use the terms “vehicle” and “client” depending on the role that we would like to emphasize.

A. The Problem: Resource Allocation for Vehicular FL

We aim to minimize the objective

$$\begin{aligned} \text{cost} = & \text{training loss} + \text{overall latency} \\ & + \text{channel usage} \end{aligned} \quad (\text{OBJ})$$

associated with an FL task, where the training loss measures the performance (accuracy) of the globally learned model, the overall latency is the total time used to train the model, and the channel usage refers to the time during which the channel is used to transmit the local models from the clients.

The space of intervention that we consider encompasses three aspects. The first one concerns *scheduling the clients* during training. Due to the limited nature of communication and computation resources, it is typically infeasible for all the clients to transmit their local model at every learning round. For this reason, they need to be scheduled: at each learning round, only a subset of them is selected. A *scheduling strategy* is thus required to optimally choose which clients should update the global model at every round.

The second aspect is the amount of *local computation* performed by the scheduled clients (vehicles). To ensure convergence of an FL algorithm to an accurate global model, the clients must carefully choose how many stochastic gradient descent (SGD) steps to perform when updating their local model. Under client scheduling, and if the clients independently choose their number of local steps at each round, optimally tuning the number of such local steps is challenging because of the combinatorial nature of the associated optimization problem.

The third aspect that we optimize for is the *transmission of local models* from the vehicles to the edge server. In general, sending the updated local models as soon as the local computations are performed (greedy behavior) would yield the fastest training. However, this strategy does not take into account the channel status, which depends on mobility and radio channel dynamics. It descends that a *greedy* transmission behavior is not necessarily optimal in terms of making the best possible use of the available channel resources. The proposed policy is mobility and channel aware; through its use, channel resources are more profitably exploited. This leads to benefits in terms of reduced transmission energy and additional room for other users or tasks that also need to exploit wireless transmissions.

B. The Solution: VREM-FL

To minimize the cost (OBJ) in a vehicular scenario, we propose Vehicular REM-based Federated Learning (VREM-FL), a co-design that jointly optimizes the threefold decision-making introduced above. An intuitive description of our co-design algorithms is illustrated in Fig. 1. In this section, we provide a high-level overview of how VREM-FL works and defer the detailed explanation to Section VI.

VREM-FL is run at the beginning of each learning round and consists of three phases, which correspond to the boxes in Fig. 1.

During the *centralized optimization* phase (top box), the edge server (*i.e.*, the orchestrator) computes the number of local steps that all the vehicles should perform to achieve the fastest training convergence and broadcasts this information. This computation uses a proxy for global convergence assuming that all the scheduled vehicles run the same number of local steps [50]. Hence, the server does not need to know the vehicles' local cost functions. This phase is formalized in Section VI-A.

In the *local customization* phase (middle box), each vehicle adjusts the number of local steps based on a local convergence criterion to trade local training speed for global accuracy. Hence, the vehicle optimizes the communication of the local model by opportunistically delaying its transmission, seeking the best trade-off between the cost components overall latency and channel usage, see (OBJ). To perform this optimization, the vehicle leverages knowledge of (i) the channel quality via the availability of an estimated REM and (ii) its planned trajectory, as explained in Section VI-B. No training is performed at this stage: instead, the choice of computation and communication is used in the following phase to discern which vehicles are the best candidates to be scheduled at the current round.

Finally, in the *centralized scheduling* phase (bottom box), the edge server receives from all the vehicles their estimated costs for participating in the round. These costs depend on the local decision-making performed during the previous phase and are suitably combined with global information available at the server, which measures the fairness of updates among the vehicles. The latter element, in the form of a combination of AoI and scheduling frequency metrics, ensures appropriate participation of all the vehicles throughout the training. The algorithm executed at the server to make scheduling decisions is described in Section VI-C.

IV. SYSTEM MODEL

In this section, we present the setup considered throughout the article. In Section IV-A, we introduce an FL task solved by vehicles that move within an urban environment served by edge servers. In Section IV-B, we describe the model that expresses channel quality experienced by the vehicles, that they use to locally assess whether they should join a round and optimize their subsequent transmissions to the server.

A. Vehicular Federated Learning

We consider N vehicles that move within an urban environment. The set of all vehicles is denoted by $\mathcal{V} \doteq \{1, \dots, N\}$, and a vehicle in this set is referred to as $v \in \mathcal{V}$. The mobility area is served by N_{bs} 5G BSs. As vehicles travel, they collect data to improve the efficiency of the tasks of interest, such as the semantic segmentation of the surrounding environment for local navigation or some global route optimization based on real-time traffic information. We label the local dataset of vehicle v as \mathcal{D}_v . To efficiently learn complex tasks from locally gathered data, all vehicles in \mathcal{V} are connected to an edge server running an FL algorithm. This allows different vehicles to cooperatively learn a common machine learning (ML) model without having to upload the collected data to the server, which may be impractical due to the high data volume or undesirable due to privacy concerns.

The FL task is described by the following optimization problem:

$$\underset{\theta \in \Theta}{\text{minimize}} \quad \mathcal{L}(\theta) \doteq \ell(\theta; \{\mathcal{D}_v\}_{v \in \mathcal{V}}) + \lambda \|\theta\| \quad (\text{FL})$$

where θ is the model parameter, function $\ell(\cdot; \cdot)$ is the empirical loss that depends on the dataset, norm $\|\theta\|$ is a regularization term that, in words, penalizes “complex” models, and λ is the regularization weight. In the following, we refer to the total cost $\mathcal{L}(\theta)$ as (regularized) loss for the sake of simplicity. Also, the size of the parameter θ amounts to B [bit].

While our co-design algorithms are agnostic to the specific algorithm used to solve problem (FL), in the following, we assume that the edge server runs FedAvg [13] and that the vehicles train their local models via gradient descent (GD) or SGD, to ground the discussion. A high-level snippet of vanilla FedAvg (without client scheduling) is provided in Algorithm 1, where all clients perform H SGD steps for each local update. We refer to a cycle composed of local updates and global aggregation (Lines 2 to 6) as a (*learning*) *iteration* or (*learning*) *round*, whose duration coincides with the time interval between two consecutive updates of the global model, and assume that the edge server runs FedAvg for T rounds in total. Moreover, we denote the global parameter at iteration t by θ^t , while the locally updated parameter of vehicle v during round t (before transmission to the aggregator) is denoted by $\theta_{v,t+H}^t$.

As commonly done in the literature, we further assume that each learning iteration has a deadline after which the global aggregation is executed regardless of the status of local updates, and a new learning round begins afterward. Also, time is slotted into slots of duration τ [s], which we consider the finest granularity to allocate resources in a time-varying fashion. In our present work, local training (Line 4) and transmission of local models from the vehicles to the server (Line 5) are addressed: we further assume that the vehicles have a deadline of K_{max} [s] to update their local models and to upload them to the server at every round, corresponding to $\lfloor K_{\text{max}}/\tau \rfloor$ time slots. We denote the set of time slots available during iteration t by \mathcal{K}_t . In the following, we will refer to the local training performed by the vehicles as *computation* to highlight the allocation of computational resources.

Algorithm 1: Vanilla FedAvg [13]

Input: Loss \mathcal{L} , rounds T , parameter θ^0 , local steps H .

Output: Learned parameter θ^t .

```

1 for  $t = 0, 1, \dots, T$  do
2   server broadcasts global parameter  $\theta^t$  to vehicles;
3   foreach vehicle  $v \in \mathcal{V}$  do
4     train local model:  $\theta_{v,t+H}^t \leftarrow \text{SGD}(\theta^t, H; \mathcal{D}_v)$ ;
5     transmit local parameter to server;
6   server aggregates local models:
    $\theta^{t+1} \leftarrow \sum_{v \in \mathcal{V}} w_v \theta_{v,t+H}^t$ ;

```

Remark 1 (Performing FL on traveling vehicles). The related literature [2], [51] remarks that the sensing capabilities of autonomous vehicles may generate GBs of data per second. The cost for such a massive amount of data is high in terms of

energy consumption and storage capacity. Hence, besides the possible need to learn a model as they travel, the vehicles may destroy the collected data right after using it for training, to save memory. Conversely, running the FL task on idle vehicles after they have collected all data imposes high, if not impractical, storage requirements and energy consumption.

B. Radio Environment and Bitrate

The area served by the BSs features a heterogeneous channel quality depending on the network coverage at different geographical locations. An REM is a database that links a (quantized) geographical location to the (estimated) value of some channel quality metric. In this work, we are interested in utilizing the knowledge of the average bitrate associated with a location $x \in \mathbb{R}^2$. We consider an REM that contains information about the SINR experienced on average across space. Given a wireless transmission setting and a geographical location x , the value of the SINR associated with x contained in the REM can be used to infer the expected average bitrate experienced by a user located at x . This information is crucially used for resource orchestration by VREM-FL. Formally, we express the location-to-bitrate map as follows. Given a vehicle v located at x_t^v at time t , the corresponding estimated average bitrate h_t^v is

$$h_t^v = \beta(\gamma(x_t^v), \eta_t^v), \quad (1)$$

where $\gamma(\cdot)$ is the location-to-SINR map encoded by the REM, $\beta(\cdot)$ is the SINR-to-bitrate map, and η_t^v is the bandwidth used by vehicle v at time t . Without loss of generality, in the rest of the paper, we set $\eta_t^v = \eta$, constant and identical for all vehicles.

In practice, we assume that an REM of the environment is computed *a priori* by means of some estimation technique [52], [53], [54] and is deployed at the edge server that broadcasts this information to the vehicles. Because REMs are approximately constant over time, as previously mentioned, we assume that an REM is sent to the vehicles only once before the FL training.

As they travel, vehicles may experience a different channel quality according to their location. We assume that the routes traversed by the vehicles are planned in advance (at least partially) so that they know their trajectory in the near future at each point in time. Specifically, at time t , vehicle v knows the locations it is about to traverse over the next D time instants, denoted by x_t^v, \dots, x_{t+D}^v , for some suitable time horizon D . This geographical information can be converted to the average bitrate experienced by the vehicle along its planned trajectory as per (1), resulting in h_t^v, \dots, h_{t+D}^v , where $h_k^v = \beta(\gamma(x_k^v), \eta)$. This information is used in our resource-allocation algorithms, as detailed in Section V.

V. PROBLEM FORMULATION

We now formalize the computation-scheduling co-design problem that is the core of our novel contribution: we first define the design parameters corresponding to the considered decision-making (Section V-A), and then formally write the objective function (OBJ) along with the overall optimization problem (Section V-B).

A. Design Parameters

Given problem (FL) and an algorithm to solve it (FedAvg), we are concerned with the threefold decision-making associated with the algorithm workflow discussed in Section III-A, which is our space of intervention.

1) *Scheduling*: First, we design a *scheduling strategy* to select the vehicles that participate in each learning iteration. Scheduling is needed because the total amount of vehicles involved in an FL task is typically large and cannot be handled at once due to the limited communication resources available at the BSs. It descends that only a (small) fraction of the vehicles can be simultaneously served through the available bandwidth to ensure an acceptable quality of service. We denote the subset of vehicles that participate in round t by $\mathcal{V}_t^S \subset \mathcal{V}$ and the maximum number of vehicles that can be scheduled in round t by $M_t^S < N$, with $|\mathcal{V}_t^S| \leq M_t^S$.

2) *Computation*: For each vehicle scheduled in a learning round, we consider two aspects for co-design. First, we allocate the amount of *computation at the vehicle*, that is, the number of descent steps (of GD or SGD) that the vehicle performs during that round to train the local model. Through a careful choice of the number of local steps, we can effectively trade convergence speed of FedAvg for the quality of the final global model. For each time slot $k \in \mathcal{K}_t$ available during iteration t , we denote by $a_k^v \in \{0, 1\}$ the *computation decision* of vehicle v for slot k : if $a_k^v = 1$, it means that v performs a batch of local steps during slot k , otherwise no computation is carried out in that slot. All slots used by vehicle v for local training during round t are denoted by $T_{\text{cpu},t}^v \doteq \sum_{k \in \mathcal{K}_t} a_k^v$. To make the training meaningful, we allocate at least $T_{\text{cpu}}^{\min} \geq 1$ slots for computation at every round.

3) *Communication*: After a vehicle has updated its local model, we optimize the *transmission from vehicle to server*. Although the training time for FL is trivially minimized if local models are immediately transmitted, in this work we are additionally interested in an efficient allocation of network resources. This allows us to save on the number of slots during which the channel bandwidth is reserved for FL and also to reduce the transmission energy. In particular, we assume that all vehicles have a constant transmission power so that optimizing for communication resources is equivalent to transmitting where the SINR is high. Similarly to computation decisions, we denote by $b_k^v \in \{0, 1\}$ the *transmission decision* of vehicle v in slot k : if $b_k^v = 1$, it means that v uses channel slot k to transmit its local model to the server, otherwise no transmission occurs during that slot. The total time used by vehicle v to transmit its local model during round t is denoted by $T_{\text{tx},t}^v \doteq \sum_{k \in \mathcal{K}_t} b_k^v$. Further, we denote by K_t^v the total amount of time elapsed from the beginning of the local model update to the end of its transmission to the server, which we refer to as *round latency* of vehicle v .

B. Optimization Problem

We aim to jointly optimize the three potentially contrasting objectives in (OBJ). As discussed above, the optimization of computation and scheduling resources enhances the final training loss and overall latency of the FL task, while optimizing communication resources translates into an efficient

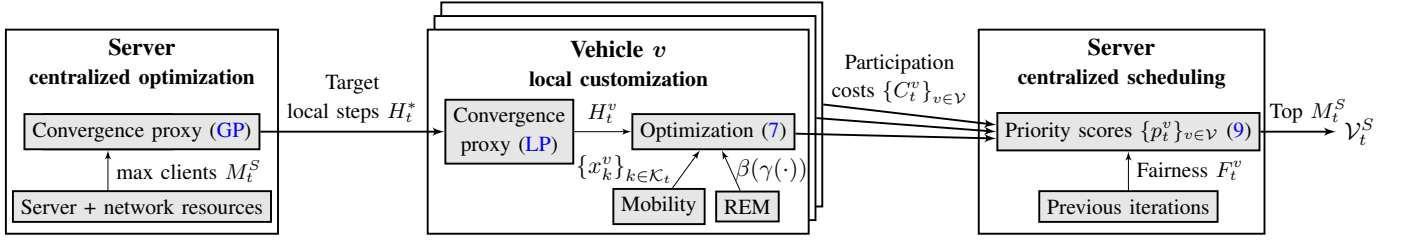


Fig. 2. **Workflow of VREM-FL.** At the beginning of learning iteration t , the server runs *centralized optimization* and transmits the globally optimal local steps to the clients. Then, each vehicle locally runs *local customization* to fine-tune computation and communication resources to be used in the round. Finally, the server performs *centralized scheduling* taking into account both feedback from the vehicles and global participation information.

channel usage during training. We now formally express these concurrent costs highlighting the dependency on the design parameters.

With a slight abuse of notation, we express the training loss as a function of both computation and scheduling (note that it also depends on the final parameters learned by FedAvg, θ^T):

$$\text{training loss} = \mathcal{L} \left(\left\{ \mathcal{V}_t^S, \{a_t^v\}_{v \in \mathcal{V}_t^S} \right\}_{t \in \mathcal{T}}; \theta^T \right), \quad (\text{TL})$$

where $a_t^v \doteq \{a_k^v\}_{k \in \mathcal{K}_t}$ denotes all the computation decisions of vehicle v throughout round t and the set $\mathcal{T} \doteq \{1, \dots, T\}$ gathers all learning rounds. The overall latency is upper bounded by TK_{\max} but can vary depending on (i) how computation and communication resources are allocated, and (ii) the channel quality experienced by the scheduled vehicles. We formalize this as

$$\text{overall latency} = K \left(\left\{ \{a_t^v, b_t^v; h_t^v\}_{v \in \mathcal{V}_t^S} \right\}_{t \in \mathcal{T}} \right), \quad (\text{OL})$$

where $b_t^v \doteq \{b_k^v\}_{k \in \mathcal{K}_t}$ and $h_t^v \doteq \{h_k^v\}_{k \in \mathcal{K}_t}$ denote all the transmission decisions of vehicle v and bitrate values experienced by v during round t , respectively. Finally, we quantify the channel usage as the time (number of slots) in which vehicles reserve the channel bandwidth to upload their local models to the server. Since this quantity depends on both the transmission decisions and the bitrate, we write it as

$$\text{channel usage} = \sum_{t \in \mathcal{T}} \sum_{v \in \mathcal{V}_t^S} T_{\text{tx},t}^v(b_t^v; h_t^v). \quad (\text{CU})$$

The total cost (**OBJ**) addressed in our co-design amounts to

$$\begin{aligned} \text{cost}(\mathcal{V}^S, a, b; h, \theta^T) &= \mathcal{L}(\mathcal{V}^S, a; \theta^T) \\ &+ (1 - w_{\text{tx}})K(a, b; h) \\ &+ w_{\text{tx}} \sum_{t \in \mathcal{T}} \sum_{v \in \mathcal{V}_t^S} T_{\text{tx},t}^v(b_t^v; h_t^v) \end{aligned} \quad (2)$$

where $\mathcal{V}^S \doteq \{\mathcal{V}_t^S\}_{t \in \mathcal{T}}$ denotes the full client schedule, $a \doteq \{\{a_t^v\}_{v \in \mathcal{V}_t^S}\}_{t \in \mathcal{T}}$, $b \doteq \{\{b_t^v\}_{v \in \mathcal{V}_t^S}\}_{t \in \mathcal{T}}$, and $h \doteq \{\{h_t^v\}_{v \in \mathcal{V}_t^S}\}_{t \in \mathcal{T}}$ collect all the computation and transmission decisions, and bitrate values associated with the scheduled vehicles across rounds. The weight $w_{\text{tx}} \in [0, 1]$ trades overall latency (**OL**) for channel usage (**CU**): if $w_{\text{tx}} = 0$, only the training time is penalized in (2); if $w_{\text{tx}} = 1$, latency is not addressed, but the usage of network resources is discouraged. Note that the performance term (**TL**) and the

TABLE I
LIST OF SYMBOLS USED IN THIS ARTICLE.

\mathcal{V}	set of vehicles
B [bit]	size of model parameter θ
τ [s]	duration of one time slot
K_{\max} [s]	maximum latency of every learning iteration
T_{cpu}^{\min}	minimum number of computation slots at every iteration
\mathcal{K}_t	set of time slots available for iteration t
s_v	local steps that vehicle v runs in one time slot
a_k^v	computation decision of vehicle v for slot k
b_k^v	transmission decision of vehicle v for slot k
$T_{\text{cpu},t}^v$	number of computation slots of vehicle v in iteration t
$T_{\text{tx},t}^v$	number of transmission slots of vehicle v in iteration t
h_k^v [bit/s]	bitrate experienced by vehicle v in slot k
B_t^v [bit]	bits that vehicle v transmits during iteration t
K_t^v [s]	latency of vehicle v in iteration t
\mathcal{V}_t^S	set of vehicles scheduled for iteration t
M_t^S	maximum number of vehicles scheduled for iteration t

latency cost (**OL**) in (2) jointly depend on all scheduled clients, whereas the resource-related cost (**CU**) decomposes linearly across them.

Equipped with the mathematical definition (2) of (**OBJ**), we are now ready to formalize the computation-scheduling co-design problem tackled in the rest of this work.

Problem 1 (Optimal computation-scheduling co-design for vehicular FL). Given (i) a set of vehicles \mathcal{V} , (ii) an REM of the environment γ , (iii) an FL algorithm, (iv) model parameters $B, K_{\max}, T_{\text{cpu}}^{\min}$, find (1) a vehicle schedule \mathcal{V}^S , (2) computation decisions a , (3) transmission decisions b , so as to optimize FL training and transmission resources:

$$\begin{aligned} (\text{P}) \quad & \arg \min_{\mathcal{V}^S, a, b} \quad \text{cost}(\mathcal{V}^S, a, b; h, \theta^T) & (\text{Pa}) \\ & \text{subject to} \quad K_t^v \leq K_{\max} \quad \forall v \in \mathcal{V}_t^S, t \in \mathcal{T}, & (\text{Pb}) \\ & \quad \quad \quad T_{\text{cpu},t}^v \geq T_{\text{cpu}}^{\min} \quad \forall v \in \mathcal{V}_t^S, t \in \mathcal{T}. & (\text{Pc}) \end{aligned}$$

In words, constraint (**Pb**) ensures that each round ends within

the pre-assigned deadline, and constraint (Pc) requires the scheduled vehicles to perform a minimal number of descent steps. The meaning of all symbols is provided in Table I.

In the next section, we propose co-design algorithms to solve Problem 1 that crucially rely on vehicular mobility and the REM to estimate the channel quality experienced by vehicles.

VI. ALGORITHMS FOR CO-DESIGN

The computation-scheduling co-design problem (P) requires designing both the local operations performed by the vehicles (computation and transmission) and the global scheduling decisions the edge server makes (the selection of which vehicles contribute in the current round). To efficiently tackle it, we propose a cascade procedure that is executed at the beginning of each round t , involving three phases (split between the edge server and the vehicles).

Centralized optimization: the edge server computes the optimal number of local steps H_t^* to be performed by the vehicles in round t and broadcasts them this value.

Local customization: the vehicles locally customize their number of local steps and their transmission pattern (the channel slots to use for sending their local model update), and send back to the server their predicted cost C_t^v to participate in round t .

Centralized scheduling: the server receives all the costs C_t^v and uses both such local information and global knowledge about the fairness of updates to select the subset of vehicles that will actually take part in the model update at round t .

Figure 2 provides a schematic representation of the workflow of VREM-FL with the three phases listed above. In the following, the operations of VREM-FL are described in detail.

A. Centralized Optimization

In this phase, the edge server first sets the maximum number M_t^S of vehicles that are allowed to participate in round t based on its available local resources (e.g., transmission channel resources and computational capability for model aggregation). Then, the server computes an approximate number of local steps to be performed by the scheduled vehicles in order to speed up the training. To evaluate at runtime the relation between the number of local steps at the vehicles and the training time, we use the proxy for *global FL convergence* proposed in [50, Eq. (1)]. This proxy assumes that M clients are scheduled at every round, and that each of them performs H local steps at every local update. The proxy is expressed as

$$T\epsilon \cong \Gamma(H, M) \doteq \frac{C}{H} + \left(1 + \frac{1}{M}\right) H \quad (\text{GP})$$

where ϵ is the estimated accuracy in T rounds, i.e., $\mathcal{L}(\theta^T) \leq \epsilon$, and C is a constant that depends on the data distribution.

The server homogeneously chooses H_t^* as the minimizer of the proxy (GP) with respect to H , setting $M = M_t^S$ and assuming that all vehicles run H_t^* local steps at all iterations:

$$H_t^* = \arg \min_H \Gamma(M_t^S, H). \quad (4)$$

This first unconstrained subproblem is convex because the objective cost (GP) is convex in H . Its solution, attainable in

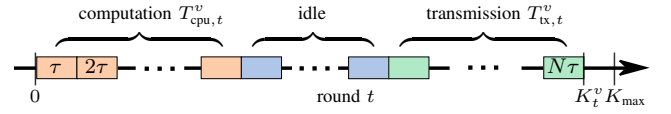


Fig. 3. **Behavior of a selected client at each round.** If a client v is selected by the server, it goes through the following steps. Each slot has duration τ [s]. At first, the client performs some local (S)GD steps (*computation*) according to its computation allocation. Eventually, it transmits its updated local model (*transmission*) after time K_t^v and within the maximum allowed latency K_{\max} , possibly waiting for some time slots (*idle*) to enjoy a better channel quality.

closed form, is

$$H_t^* = \sqrt{\frac{C}{\left(1 + \frac{1}{M_t^S}\right)}}. \quad (5)$$

This also reveals the dependency of the optimal number of local steps H_t^* on the number of scheduled clients: it is a strictly increasing and concave function of M (for $M \geq 1$) which saturates to \sqrt{C} for $M \rightarrow +\infty$ (horizontal asymptote).

After computing H_t^* , the server broadcasts this value to all the vehicles for the second phase.

B. Local Customization

In this phase, each vehicle independently executes a local subroutine to allocate slots for computation and communication. This allocation attempts to optimize (i) convergence of local training and (ii) channel utilization. The resulting number of local steps is temporarily stored by the vehicles, which use it later to perform the local model update in case they are actually scheduled. If a vehicle has a means to (efficiently) estimate the loss gradient, it first refines the number of local steps H_t^* communicated by the server (*computation refinement*) based on a proxy for local convergence, obtaining a new number of local steps H_t^v , and then it optimizes for transmission (*communication optimization*). Instead, if evaluating the gradient is expensive, the vehicle skips the computation refinement at this stage and sets the number of local steps as $H_t^v = \max\{H_t^*, s_v T_{\text{cpu}}^{\min}\}$.

1) *Computation refinement:* To optimize the local updates of the vehicle, we consider a local proxy that jointly keeps into account the individual client convergence properties and the global recommendation H_t^* indicated by the server. As such, the proxy is obtained as the sum of multiple terms. First, we consider a "convergence" proxy $\Theta_t^v(H_t^v)$ related to the local optimality gap, which bounds the client deterministic gradient norm after H_t^v local steps of gradient descent starting from the global parameter θ^t :

$$\|\nabla \ell^v(\theta_{t,t+H_t^v}^v)\| \leq \Theta_t^v(H_t^v) \doteq \|\nabla \ell^v(\theta^t)\| (1 - \kappa_v^{-1})^{H_t^v - 1}. \quad (\text{LP})$$

The constant $\kappa_v > 0$ is the condition number associated with the local loss ℓ^v . The proxy (LP) is based on quadratic cost functions, and we derive it explicitly in Appendix A. The proxy (LP) is motivated by the fact that the optimality gap $\|\theta - \theta^*\|$ is in general proportional to the gradient norm, but we have only access to the gradient, while θ^* is unknown. It can be computed by each client based on their local cost only and does not take into account the distributed nature of the FL problem. Hence, during this step, the vehicle v refines its

computation by solving the optimization problem

$$H_t^v = \arg \min_{H \in \mathbb{N}} \quad \Theta_t^v(H) + \frac{\rho_1 H}{\|\nabla \ell^v(\theta^t)\|} + \rho_2 (H - H_t^*)^2 \quad (6a)$$

$$\text{subject to} \quad H \geq s_v T_{\text{cpu}}^{\min}. \quad (6b)$$

The second addend in (6a) accounts for how close the vehicle is to a local minimum, forcing few steps if the vehicle has (locally) almost converged and many steps if it is still far from convergence, whereas the third addend encourages the chosen local steps H_t^v to be similar to the target H_t^* computed by the server. Note that the cost function (6a) is convex in H and grows unbounded as $H \rightarrow +\infty$, so that problem (6) can be efficiently solved by a linear search. The number of computation slots is then set as $T_{\text{cpu},t}^v = \lceil H_t^v / s_v \rceil$. For the sake of simplicity, but without loss of generality, we require that the vehicle allocates all slots for computation at the beginning of the round. Formally, this means $a_k^v = 1$ for $k = 1, \dots, T_{\text{cpu},t}^v$ and $a_k^v = 0$ for $k > T_{\text{cpu},t}^v$ for all $k \in \mathcal{K}_t$. These are the “computation” leftmost slots in Fig. 3.

2) *Communication optimization*: In this step, the vehicle chooses the time slots for the transmission of its local model to the server, adjusting the computation slots if needed. For simplicity, we require the vehicle to allocate a batch of consecutive slots also for transmission. Formally, the communication decisions for round t are $b_k^v = 0$ for $k = 1, \dots, \bar{k}_1$, and $b_k^v = 1$ for $k = \bar{k}_1 + 1, \dots, \bar{k}_2$, for some $\bar{k}_1 \geq T_{\text{cpu},t}^v$ and $\bar{k}_2 > \bar{k}_1$. The allocation of slots for computation and communication is pictorially represented in Fig. 3. Specifically, the latter set of slots with $b_k^v = 1$ needs to be enough for the vehicle to transmit its model (B [bit]) to the server by the deadline K_{max} . We denote the set of such transmission patterns by $\mathcal{B}_t^v(T_{\text{cpu},t}^v)$. To choose the communication pattern, given $T_{\text{cpu},t}^v$ slots of computation, the vehicle attempts to solve the following optimization problem:

$$b_t^v = \arg \min_{b \in \mathcal{B}_t^v(T_{\text{cpu},t}^v)} \quad C_t^v \doteq (1 - w_{\text{tx}})K_t^v + w_{\text{tx}}T_{\text{tx},t}^v \quad (7a)$$

$$\text{subject to} \quad K_t^v \leq K_{\text{max}}, \quad (7b)$$

$$B_t^v \geq B. \quad (7c)$$

The cost C_t^v in (7a) is designed to trade round latency K_t^v for channel occupancy $T_{\text{tx},t}^v$, according to the overall objective cost (2). To solve (7), vehicular mobility in conjunction with the REM plays a crucial role: each vehicle inspects the REM to estimate the available bitrate in the near future and, in turn, the number of time slots needed to upload the model. For example, if the vehicle is about to travel close to a well served area (e.g., a main urban road), it will be likely enjoying a high channel quality and thus take a short time for the upload, whereas, if it is approaching a weakly served area (e.g., a tunnel), it will predict poor channel conditions and might even declare (7) infeasible, giving up on joining the learning round. A pictorial representation of the mobility-aware REM-based evaluation of the cost (7a) is provided in Fig. 4. In this figure, for case 1, transmission slots are allocated in a greedy fashion, whereas for case 2, the client defers the transmission of the local model, waiting for the channel quality to improve. This trades some

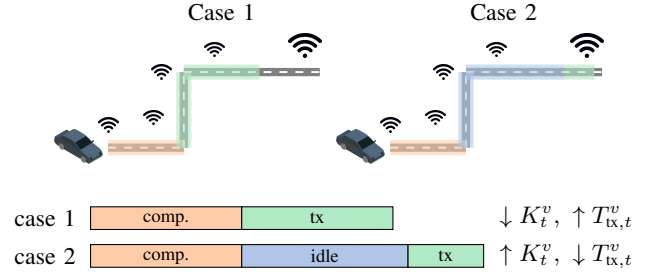


Fig. 4. **REM-based solution for communication optimization.** Two evaluations of the objective cost (7a). In Case 1, transmission occurs under poor channel conditions (low bitrate) and takes long time. On the contrary, in Case 2, idle slots delay communication until when the vehicle travels through a well served area (high bitrate), so that transmission time is shorter.

extra delay for a better utilization of channel resources.

Computation and communication decisions for the round are set by first solving (6) – if possible – to fine-tune the number of computation slots, and then (7) until a feasible computation-communication pattern is found or the whole allocation is declared infeasible. Algorithm 2 summarizes the workflow of this phase. Eventually, each vehicle v transmits its estimated cost C_t^v for participation in round t to the server, to inform the latter on the expected benefit of scheduling v for the present round. We use the convention that, if vehicle v cannot find a feasible allocation for round t (i.e., problem (7) turns out to be infeasible), it will communicate an infinite cost C_t^v , see Line 6.

Remark 2 (Computation refinement for scheduled vehicle). Even if a vehicle cannot evaluate the cost (6a) in reasonable time and skips the refinement (6), scheduled clients may refine their local steps *after* they have been scheduled. Indeed, they can compute or approximate the gradient $\nabla \ell^v(\theta^t)$ at the beginning of the round, for example by running a few descent steps, and then solve for H_t^v according to (6) with the (approximate) gradient just computed. Then, they complete the local update by running SGD until they reach H_t^v total steps.

Remark 3 (Reducing latency vs. network resources). Optimization (7) is designed so that not only the vehicles can reduce their associated latency K_t^v for round t concerning the deadline K_{max} , but also the server is aware of their expected latency. This allows to favor those vehicles that are likely to transmit their local models in a short time and in turn to speed up the whole training. This is experimentally demonstrated in Section VII via ablation studies and comparisons against standard scheduling strategies. In particular, by tuning the weight w_{tx} in (7a), a system designer can encourage a short training (small w_{tx}) or an economic usage of network resources (large w_{tx}).

C. Centralized Scheduling

After the server receives information from all vehicles about their (predicted) cost for the round, the vehicles are scheduled based on both this cost, that measures the training performance, and on fairness metrics such as the AoI and scheduling frequency, accounting for the learning accuracy of the global model. In particular, drawing inspiration from [14], we define the fairness F_t^v for vehicle v at round t as

$$F_t^v \doteq \frac{1}{\phi_t^v} + A_t^v \quad (8)$$

Algorithm 2: Subroutine `customize_local`

Input: Local proxy Θ^v , minimum computation T_{cpu}^{\min} , maximum round latency K_{\max} , target steps H_t^* .
Output: Cost C_t^v , computation and communication decisions a_t^v and b_t^v for round t .

- 1 **if** *can efficiently estimate* $\nabla \ell_t^v$ **then**
- 2 compute H_t^v as the solution to (6);
- 3 **else**
- 4 set $H_t^v \leftarrow \max \{H_t^*, s_v T_{\text{cpu}}^{\min}\}$;
- 5 set $T_{\text{cpu},t}^v \leftarrow \lceil H_t^v / s_v \rceil$;
- 6 set $C_t^v \leftarrow +\infty$;
- 7 **repeat**
- 8 compute b_t^v as the solution to (7);
- 9 **if** *problem (7) is feasible* **then**
- 10 set $C_t^v \leftarrow C_t^v(b_t^v)$;
- 11 store computation $T_{\text{cpu},t}^v$ and communication b_t^v ;
- 12 **break**;
- 13 **else**
- 14 set $T_{\text{cpu},t}^v \leftarrow T_{\text{cpu},t}^v - 1$;
- 15 **until** $T_{\text{cpu},t}^v < T_{\text{cpu}}^{\min}$;

where ϕ_t^v is the scheduling frequency of vehicle v before round t , and A_t^v is the AoI of its updates.

To schedule the participating vehicles, the server assigns a *priority score* p_t^v to each vehicle v for round t :

$$p_t^v \doteq \begin{cases} \frac{w_C}{C_t^v} + w_A F_t^v & \text{if } C_t^v < +\infty \\ -1 & \text{if } C_t^v = +\infty. \end{cases} \quad (9)$$

The weights w_C and w_A in (9) should be chosen so as to strike a balance between high-performing vehicles, which may significantly reduce the objective cost (2) in the short run, and overall training in the long run that needs to gather information from all vehicles to eventually learn an accurate global model.

Formally, the vehicles with the highest priority scores are scheduled, according to the following optimization problem:

$$\mathcal{V}_t^S = \arg \max_{\mathcal{V}^S \subseteq \mathcal{V}} \sum_{v \in \mathcal{V}^S} p_t^v \quad (10a)$$

$$\text{subject to } |\mathcal{V}^S| \leq M_t^S. \quad (10b)$$

According to our convention described in Section VI-B, the clients that communicate infeasible participation are assigned a negative priority score as per (9), which automatically excludes them from the round according to maximization of (10a).

Set \mathcal{V}_t^S contains the vehicles that the server schedules for transmitting their local updates in the current round t . The VREM-FL workflow is provided in Algorithm 3.

VII. NUMERICAL RESULTS

This results section is divided into two parts. In the first one, we use a synthetically generated dataset with non-iid data, used to train a least-squares regression problem to show in detail the operation of VREM-FL. In the second part, VREM-FL is applied to the real-world semantic segmenta-

Algorithm 3: VREM-FL

Input: Global proxy Γ , local proxy Θ^v , maximal round latency K_{\max} , minimal computation slots T_{cpu}^{\min} , maximal number of scheduled vehicles M_t^S .
Output: Scheduled vehicles \mathcal{V}_t^S .

centralized optimization (at the edge server):

- 1 compute H_t^* as the solution to (4);
- 2 broadcast H_t^* and maximal latency K_{\max} to vehicles;

local customization (at the vehicles):

- 3 **foreach** vehicle $v \in \mathcal{V}$ **do**
- 4 $C_t^v \leftarrow \text{customize_local}(\Theta^v, T_{\text{cpu}}^{\min}, K_{\max}, H_t^*)$;
- 5 send C_t^v to server;

centralized scheduling (at the edge server):

- 6 **foreach** vehicle $v \in \mathcal{V}$ **do**
- 7 compute p_t^v as per (9);
- 8 populate \mathcal{V}_t^S according to (10);
- 9 **return** \mathcal{V}_t^S .

tion dataset ApolloScape [12], to test the algorithm on a task of specific interest for vehicular applications. The state-of-the-art deeplabv3 [55] model is trained, choosing mobilenetv3-large [56] as a backbone.

A. Mobility and Urban Radio Environment Generation

The simulation environment is implemented in Python, downloading the map of the city of Padova (Italy) from OpenStreetMap [57] and using SUMO [9] to simulate 1000 vehicles that move across the city for one hour. The first 10 minutes of simulation are discarded to let the road map populate with a sufficiently large number of vehicles.

On top of the city map, BSs are deployed with an inter-site distance of 600 m, according to typical 5G deployment criteria. Average SINR values and the corresponding bitrates have been obtained through the Matlab 5G NR link-level simulation tool [58]. SINR values are calculated considering (i) the transmission power of vehicles, (ii) physical settings of the 5G NR, (iii) propagation models, and (iv) interference and noise power. We set the transmission power of vehicles to 23 dBm. Without loss of generality, we assume to allocate (in the frequency domain) a fixed number of 10 resource blocks for data transmission. Carrier frequency is set to 3.5 GHz. The sub-carrier space and the resulting size (in the frequency domain) of each single radio resource block are set to 30 kHz and 360 kHz, respectively. Hence, the per-client bandwidth for 10 resource blocks is $\eta = 3.6$ MHz (see (1)). The antenna height of BSs and vehicles is set to 25 m and 1.5 m, respectively. Path loss parameters are set according to the urban microcell scenario, as defined in the TR 38.901 specification of 3GPP. The slow-fading (shadowing) is added to the coverage area of each BS following the 3GPP guidelines [59], with a decorrelation distance of 25 m and standard deviation of 6 dB, which are common values for urban environments [60]. Finally, the noise figure, used to derive the noise power, is set to 6 dB. The bitrate corresponding to a given SINR average value – *i.e.*, the map $\beta(\cdot)$ in (1) – is obtained according to the physical uplink shared channel (namely 5G NR PUSCH)

TABLE II
LIST OF THE PARAMETERS USED FOR THE SIMULATIONS.

$T = 50$ min	simulation horizon
$\tau = 1$ s	duration of one time slot
$K_{\max} = 100$ s	maximum latency of every iteration
$T_{\text{cpu}}^{\min} = 1$	minimum computation slots
$M_t^S = 30$	maximum number of vehicles scheduled
$\rho_1 = 0.001, \rho_2 = 1$	weight coefficients of Eq. (6)
$C = 200$	weight coefficient of Eq. (GP)
$w_C = 1, w_A = 0$	weight coefficients of Eq. (9)

throughput experienced in a 5G New Radio link [61], [62], [63] for that value of SINR. In particular, the average throughput is calculated through the Matlab 5G NR link-level simulation tool implementing the 3GPP NR standard [58], assuming that vehicles experience a given average SINR value during the time slot τ of 1 s.

B. Synthetic Dataset Generation

We consider a linear data generator in which data points are vectors in \mathbb{R}^n . To build the generator, we consider a set \mathcal{U} of n linearly independent basis vectors, $\mathcal{U} = \{u_1, \dots, u_n\}$. We scale these vectors by constants $\sigma_1, \dots, \sigma_n$ that take values between 10^{-2} and 1. The resulting generating set of vectors is $\tilde{\mathcal{U}} = \{\tilde{u}_1, \dots, \tilde{u}_n\} = \{\sigma_1 u_1, \dots, \sigma_n u_n\}$. Each synthetic data sample x is generated by a random linear combination of the form $x = \sum_{j=1}^n z_j \tilde{u}_j$, where z_1, \dots, z_n are i.i.d. Gaussian random variables. We generate S data samples. Accordingly, S response values y_1, \dots, y_S are generated from the data samples x_1, \dots, x_S as $y_i = x_i^T \theta^*$, where the generating parameter θ^* is also obtained as a random linear combination of $\{\tilde{u}_1, \dots, \tilde{u}_n\}$. For this synthetic dataset, we study regularized least squares, *i.e.*, the instantiation of (FL) with loss function $\ell(\theta) = \sum_{i=1}^S (\theta^T x_i - y_i)^2$ and regularization term $\lambda \|\theta\|^2$, where $\lambda > 0$ is the regularization parameter. For the purpose of the ablation study with synthetic data, we set a small parameter dimension $n = 25$. Accordingly, to get meaningful results with respect to the scheduling design, we rescale the bitrate values by a factor 2×10^{-5} .

C. Performance Using Estimated REMs

We show the performance of VREM-FL on the synthetic dataset described in Section VII-B when the REM is estimated via Gaussian Process Regression (GPR) [8], [11] performed on a limited number of measurements. We consider the cases where 100, 150, or 250 measurements are available in each BS cellular sector. For each sector, we select the measuring locations uniformly at random. To perform GPR, we assume that the standard deviation and the de-correlation distance of the shadowing process are known *a priori*.¹ The parameters used in the simulations for FL and VREM-FL settings are, unless differently specified, those reported in Table II.

In Fig. 5, we show the distance from the optimal parameter

¹If this is not the case, they can be estimated via standard techniques [8].

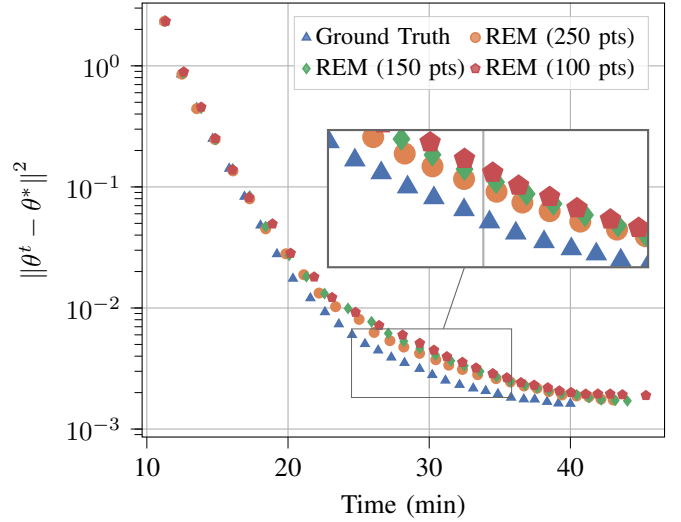


Fig. 5. Performance of VREM-FL with the synthetic dataset (see Section VII-B) considering estimations of the REM map obtained by varying the granularity of available measures.

θ^* of the least squares problem as a function of the simulation time, where different lines denote a different number of measures available to generate the REM maps through GPR. Markers denote the simulation slot where the server has received all the updates from the clients and computes the average, *i.e.*, the end of a learning round. Triangular blue markers correspond to the ground truth, namely, the real REM is available at the scheduler. As it can be seen, it is in general true that the more points are available to generate the REM estimation, the more likely it is to avoid stragglers. Stragglers are those nodes that slow down the learning process because they do not have sufficient computational or communication resources. In the case under analysis, the presence of scheduled nodes that had an estimated channel quality superior to the real one makes the learning round last longer, hence the total latency increases. We observe that the estimated map obtained using 100 points produces a total learning duration approximately 5 minutes longer than the ground truth and 2 minutes longer than the estimated map with 250 points. For the rest of the experiments, we used the REM estimated with 250 points.

D. Comparison with Other Scheduling Policies

VREM-FL is compared with three scheduling benchmarks:

- Random:** Clients are chosen by sampling them randomly with equal probability (uniform random variable) [13].
- Round robin:** Clients are chosen by the scheduler based on a round robin policy, *i.e.*, are selected in a cyclic order.
- Fairness only:** This is the scheme obtained by optimizing the metric proposed in [14]. This is equivalent to VREM-FL by setting $w_C = 0$ in (9), *i.e.*, the scheduling priority is computed as $p_t^v = F_t^v$. A crucial difference between this method and VREM-FL is that the cost C_t^v is unused and thus the two cases in (9) are indistinguishable: even if a vehicle would be able to report an infinite participation cost, this information is neglected by “Fairness only” that uses only fairness-related information F_t^v .

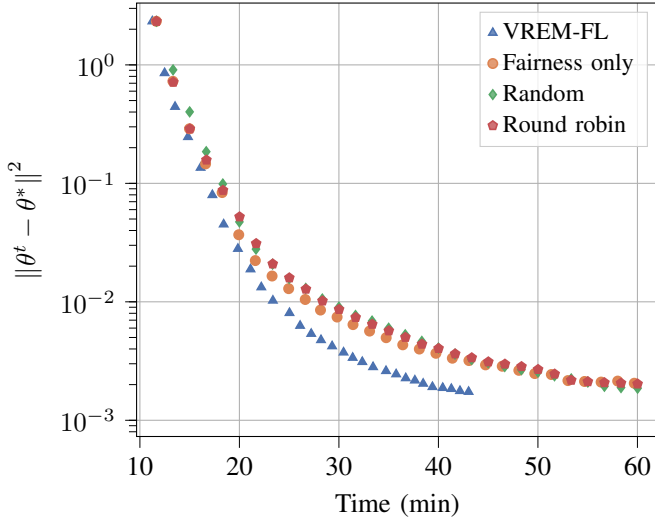


Fig. 6. Comparison between VREM-FL and the considered benchmarks in terms of client selection algorithm, with the synthetic dataset (see Section VII-B). Model convergence as a function of time.

The comparison is shown in Fig. 6. The “Random” and “Round robin” scheduling methods perform very similarly: the learning process converges, but it takes longer than the other two algorithms. The target of 30 rounds is not even reached along the simulation horizon of 50 minutes. Also using the “Fairness only” approach the whole simulation horizon is needed. Nonetheless, a slight advantage in the model performance can be observed at early stages because the information is integrated in a more intelligent way, ensuring that all vehicles contribute evenly. Notably, under the given settings, VREM-FL can reduce the total latency by at least 28% for the same model accuracy. This is achieved by a smart use of the estimated channel conditions, and employing communication resources in a wiser manner.

E. Ablation Study

We propose an ablation study to isolate the effect of the proposed local steps adaptation strategy (Fig. 7a) and transmission policy (Fig. 7b).

Specifically, from Fig. 7a we see that performing the minimum number of GD steps (*i.e.*, only one step) locally at each round results in a stable curve but slow convergence. The opposite policy “max steps” is obtained by filling all the idle slots between computation and transmission (see Fig. 3) with additional GD steps. In this way, the total latency is the same as that of our optimized solution, the local models are also transmitted in the same channel slots, but the total number of local iterations is higher than the proposed VREM-FL (labeled “adjusted steps” in the figure). In fact, the latter version might limit the number of steps executed locally based on the local and global optimization proxies. Although “max steps” is initially faster than “adjusted steps”, both solutions converge after 40 minutes (*i.e.*, approximately 25 rounds). In Fig. 7c, on the right, the normalized number of GD steps with respect to the strategy “max steps” referred to this experiment is shown. Although “min steps” uses only 6% of the total steps, its convergence is too slow. Noteworthy, “adjusted steps”

shows a gain of 28% with respect to “max steps”, which directly translates into higher energy efficiency and better usage of the computation resources, while reaching the same convergence accuracy in a comparable amount of time.

In Fig. 7b, the results relative to varying the weight w_{tx} in the optimization problem (7) are shown. Specifically, tuning w_{tx} between 0 and 1 makes the solution move along the Pareto front between the two extremes $w_{tx} = 1$ (orange circles), which corresponds to minimizing the number of slots where the channel is filled with communication, and $w_{tx} = 0$ (green diamonds), which corresponds to minimizing the total latency. The latter policy with $w_{tx} = 0$ corresponds to transmitting the local models as soon as the GD steps are completed, while the former $w_{tx} = 1$ uses the REM and waits for the best transmission window available in terms of bitrate. Any coefficients in between correspond to a weighted solution between these two criteria: as an example, we show the results for $w_{tx} = 0.5$ (blue triangles). It is evident that, as $w_{tx} \rightarrow 0$, convergence is faster, as this solution minimizes the total latency. The scenario with $w_{tx} = 0.5$ is reasonably close: it takes 2 min longer to complete the given 30 rounds, whereas setting $w_{tx} = 1$ only penalizes the usage of transmission resources and takes all the available 50 minutes. By looking at the resource usage (Fig. 7c, on the left), we see that, in our context, it is possible to reduce the number of slots used for communications by at most 21% (*i.e.*, from $w_{tx} = 0$ to $w_{tx} = 1$). Interestingly, by setting $w_{tx} = 0.5$, a gain of 11% in the resource usage metric is observed, hence improving significantly the efficiency while performing very close to $w_{tx} = 0$ in terms of overall latency.

F. Experiments with ApolloScope

In this section, the performance of VREM-FL is assessed using the real-word semantic segmentation dataset ApolloScope. Specifically, the score used is the mean intersection over union (mIoU), a popular evaluation metric for segmentation tasks, obtained first by computing the ratio between the area of the intersection between the predicted and ground truth regions by the area of their union, then by taking their average. In mathematical terms, let \mathcal{R} be the set of semantic regions, and, by denoting with $|\mathcal{R}|$ its cardinality, it holds

$$\text{mIoU} = \frac{1}{|\mathcal{R}|} \sum_{r \in \mathcal{R}} \frac{r^{\text{pred}} \cap r^{\text{true}}}{r^{\text{pred}} \cup r^{\text{true}}}. \quad (11)$$

In these simulations, the bitrate used to run VREM-FL is obtained through the estimation method of Section VII-C with 250 samples. We set the fairness regularization coefficient to $w_A = 0.01$ and modify the other optimization coefficients to reflect the different nature of the problem, setting $C = 1000$, $\rho_1 = 1$, $\rho_2 = 0.02$, and $w_{tx} = 0.9$. These choices have the effects of increasing the number of local SGD steps and inducing the system to wait for the best transmission window in the given time. The total learning horizon lasts 50 minutes and each round has a deadline of two minutes during which scheduled vehicles must update their local models and upload them to the server. The initial local learning rate is set to $\text{lr} = 2.5 \times 10^{-4}$ with a cosine annealing scheduler reducing

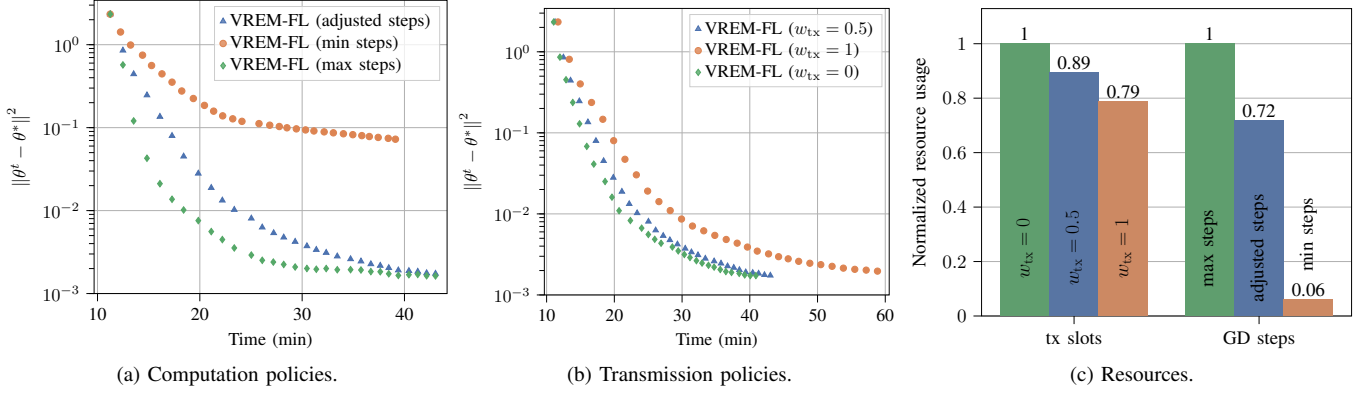


Fig. 7. Performance of the VREM-FL with the synthetic dataset (see Section VII-B) scheduler while varying the policies relative to the computation (number of GD steps) and communication (number of slots where the clients fill the channel) resources.

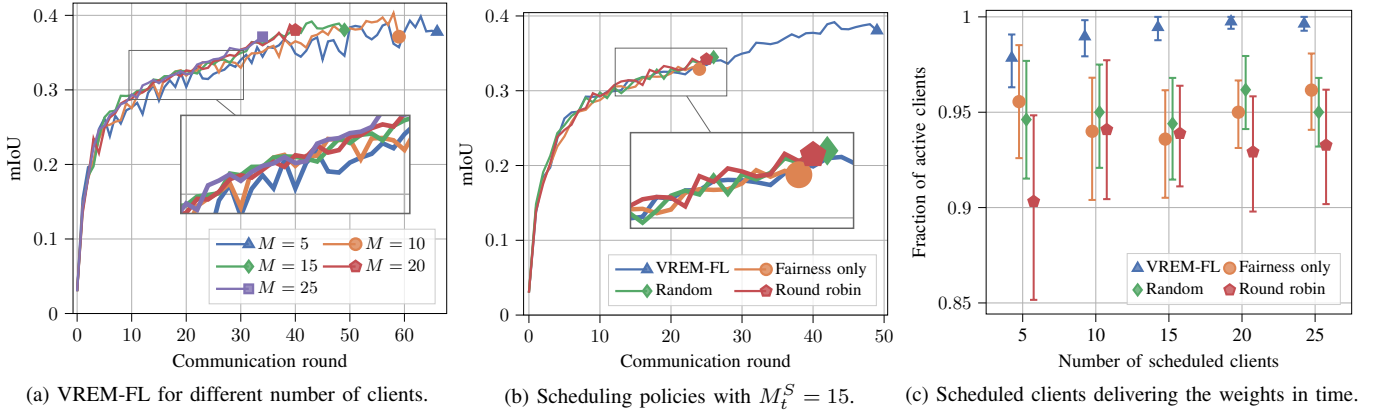


Fig. 8. Performance of VREM-FL for the real-world dataset ApolloScope concerning the benchmarks.

progressively its value and the local optimizer used is vanilla SGD. A resolution-downsampled version of ApolloScope is split assigning to the vehicles a single record session among those available to reflect the fact that data collected by vehicles is correlated in time and space. The model is trained with minibatches of size 32 considering that the rate of SGD is $s_v = 3$ steps per time slot (measured on an NVIDIA GeForce RTX 2080 GPU).

In Fig. 8a, the mIoU score of VREM-FL for different numbers of sampled clients M is plotted against the communication round. As shown, selecting fewer clients, *e.g.*, $M = 5$, gives the possibility to perform more communication rounds within the vehicular simulation horizon (one hour), as the time needed to complete a single round is short. However, the learning quality is poor, as frequent spikes are present because a low number of clients is not representative of the full dataset, which may vary a lot across rounds. On the other hand, by increasing the number of clients, the learning quality stabilizes, but, *e.g.*, for $M = 25$ we pay this stabilization in terms of longer round duration. Actually, scheduling more clients means increasing the probability that at least one of them behaves as a straggler, *i.e.*, taking longer to transmit the parameters to the server, and this results in a reduced latency efficiency. By looking more in detail at the zoomed area, we can see that learning stabilizes for $M \geq 15$, which provides a better latency behavior if compared to using $M > 15$. Hence, for the following results,

we consider $M = 15$ as the best tradeoff between learning quality and latency.

Fig. 8b shows the comparison between VREM-FL and the benchmark scheduling algorithms. As shown, there is no significant difference in terms of quality of learning, *i.e.*, even optimizing the fairness metric does not provide advantages against the random policy in this setting. However, using VREM-FL the server is capable of aggregating the parameters at a double rate with respect to all the benchmarks. By exploiting the REM, the scheduler can choose the fastest clients to transmit their local model weights, and the system can perform 49 communication rounds instead of the 24-26 performed by the benchmarks within the same time horizon. This directly translates into a higher mIoU for the same training time – about 9.3% higher than the best benchmark strategy.

Clients that cannot send their model parameters update within the learning round deadline waste computation and, possibly, communication resources. To assess the capability of VREM-FL to prevent resources from being wasted, we evaluate the fraction of clients that upload their update to the server within the deadline, varying the number of scheduled clients (Fig. 8c). Compared to the benchmark scheduling algorithms, channel quality maps allow VREM-FL to effectively select only those clients who will send their weights in time. This result is consistent, being the variance relatively small. On the other hand, without REM availability, a drop in the share of

clients that transmit their weights is observed, with a worst-case scenario of 85% in the simulated settings. The average value of the benchmark algorithms is around 94%, while for VREM-FL is close to 100%. This demonstrates that not only VREM-FL outperforms the benchmark strategies in terms of learning performance, but it also does so with a more economical and efficient usage of computation resources at the vehicles and of communication resources at the network edge.

VIII. CONCLUSION AND FUTURE WORK

Motivated by the need of efficient solutions for FL tasks in vehicular networks, we have proposed VREM-FL, a computation-scheduling co-design algorithm that jointly optimizes a learning-related performance metric and network-related communication resources. Specifically, VREM-FL orchestrates local computations at the vehicles, transmission of their local models to the edge server, and schedules clients at each learning iteration to strike a good balance between learning accuracy, training time, and wireless channel usage. Experimental results on a synthetic LS problem and on a real-world semantic segmentation task demonstrate that VREM-FL provides superior learning performance as compared to common scheduling strategies by promoting a frugal use of computation and communication resources.

The present study focuses on the FL algorithm, client mobility is assumed to be given and non-controllable. However, future smart and autonomous vehicles may be in the position of changing their planned route to favor ancillary tasks, such as the execution of an FL algorithm or the transmission of data to roadside servers. Hence, we foresee scenarios where decision-making can be augmented via trajectory steering of (some of) the participating vehicles, to optimize even further the vehicle learning performance and their resource utilization.

APPENDIX A

ANALYTICAL DERIVATION OF LOCAL PROXY (LP)

We choose the proxy $\Theta_t^v(H_t^v)$ based on the convergence behavior of deterministic gradient descent when applied to least squares problems. For completeness, we now illustrate the explicit derivation of this proxy. Let $\ell(\theta) = \sum_{i=1}^S (\theta^\top x_i - y_i)^2 + \lambda \|\theta\|^2$ be a regularized quadratic cost function with $\lambda > 0$ (see Section VII-B). We denote by $g(\theta) = \nabla \ell(\theta) \in \mathbb{R}^n$ and $\Lambda = \nabla^2 \ell(\theta) \in \mathbb{R}^{n \times n}$ the gradient and the (constant) Hessian matrix of the cost function, respectively. Let θ^* be the unique minimizer of $\ell(\theta)$. In least squares, the gradient can be written as $g(\theta) = \Lambda(\theta - \theta^*)$ [64]. Recall that, for a constant step size $\alpha > 0$, the gradient descent update is $\theta^{t+1} = \theta^t - \alpha g(\theta^t)$ starting from the initial parameter θ^0 . Therefore, we can write

$$\begin{aligned} g(\theta^{t+1}) &= \Lambda(\theta^{t+1} - \theta^*) = \Lambda(\theta^t - \theta^* - \alpha g(\theta^t)) \\ &= g(\theta^t) - \alpha \Lambda g(\theta^t) = (I - \alpha \Lambda) g(\theta^t). \end{aligned} \quad (12)$$

Hence, the rate of convergence of $g(\theta^t)$ to zero is dictated by the largest eigenvalue (in magnitude) of $(I - \alpha \Lambda)$ that, denoting the eigenvalues of Λ by $\lambda_1 \geq \dots \geq \lambda_n > 0$, is minimized by choosing $\alpha = \frac{2}{\lambda_1 + \lambda_n}$ (see, e.g., the proof in [64, Theorem 1]). This yields a convergence factor of $\frac{\lambda_1 - \lambda_n}{\lambda_1 + \lambda_n} \leq$

$1 - \frac{\lambda_n}{\lambda_1} = 1 - \frac{1}{\kappa}$, where $\kappa = \frac{\lambda_1}{\lambda_n}$ is the condition number of the problem. Consequently, we get

$$\|g(\theta^{t+1})\| \leq \left(1 - \frac{1}{\kappa}\right)^{t+1} \|g(\theta^0)\|, \quad (13)$$

from which we derive the proxy (LP).

ACKNOWLEDGMENT

Views and opinions expressed in this work are of the authors and may not reflect those of the funding institutions.

REFERENCES

- [1] Cisco. (2020, Mar. 9) *Cisco annual Internet report 2018-2023*. Accessed on: Nov. 15, 2023. [Online]. Available: <https://www.cisco.com/c/en/us/solutions/collateral/executive-perspectives/annual-internet-report/white-paper-c11-741490.html>
- [2] Siemens. (2021, Jan. 22) *The Data Deluge: What do we do with the data generated by AVs?* Accessed on: Nov. 15, 2023. [Online]. Available: <https://blogs.sw.siemens.com/polarion/the-data-deluge-what-do-we-do-with-the-data-generated-by-avs/>
- [3] J. Konečný, H. B. McMahan, F. X. Yu, P. Richtárik, A. T. Suresh, and D. Bacon, "Federated learning: Strategies for improving communication efficiency," *arXiv e-prints*, p. arXiv:1610.05492, 2016.
- [4] A. Mitra, R. Jaafar, G. J. Pappas, and H. Hassani, "Linear convergence in federated learning: Tackling client heterogeneity and sparse gradients," *Proc. NeurIPS*, vol. 34, pp. 14 606–14 619, 2021.
- [5] M. Chen, Z. Yang, W. Saad, C. Yin, H. V. Poor, and S. Cui, "A joint learning and communications framework for federated learning over wireless networks," *IEEE Trans. Wireless Commun.*, vol. 20, no. 1, pp. 269–283, 2020.
- [6] M. Chen, H. V. Poor, W. Saad, and S. Cui, "Convergence time optimization for federated learning over wireless networks," *IEEE Trans. Wireless Commun.*, vol. 20, no. 4, pp. 2457–2471, 2020.
- [7] S. Bi, J. Lyu, Z. Ding, and R. Zhang, "Engineering radio maps for wireless resource management," *IEEE Wireless Commun.*, vol. 26, no. 2, pp. 133–141, 2019.
- [8] N. Dal Fabbro, M. Rossi, G. Pillonetto, L. Schenato, and G. Piro, "Model-free radio map estimation in massive MIMO systems via semi-parametric Gaussian regression," *IEEE Wireless Commun. Lett.*, vol. 11, no. 3, pp. 473–477, 2022.
- [9] Eclipse. (2023) *Simulator of Urban MObility*. Accessed on: Nov. 15, 2023. [Online]. Available: <https://eclipse.dev/sumo/>
- [10] A. Grassi, G. Piro, G. Boggia, M. Kurras, W. Zirwas, R. SivaSiva Ganesan, K. Pedersen, and L. Thiele, "Massive MIMO interference coordination for 5G broadband access: Integration and system level study," *Computer Networks*, vol. 147, pp. 191–203, 2018.
- [11] L. S. Muppirisetty, T. Svensson, and H. Wymeersch, "Spatial wireless channel prediction under location uncertainty," *IEEE Trans. Wireless Commun.*, vol. 15, no. 2, pp. 1031–1044, 2015.
- [12] X. Huang, X. Cheng, Q. Geng, B. Cao, D. Zhou, P. Wang, Y. Lin, and R. Yang, "The apolloscape dataset for autonomous driving," in *Proc. IEEE CVPR Workshops*, 2018, pp. 954–960.
- [13] B. McMahan, E. Moore, D. Ramage, S. Hampson, and B. A. y Arcas, "Communication-efficient learning of deep networks from decentralized data," in *Proc. AISTATS*, 2017, pp. 1273–1282.
- [14] M. E. Ozfatura, J. Zhao, and D. Gündüz, "Fast federated edge learning with overlapped communication and computation and channel-aware fair client scheduling," in *Proc. IEEE SPAWC*, 2021, pp. 311–315.
- [15] M. M. Amiri, D. Gündüz, S. R. Kulkarni, and H. V. Poor, "Convergence of update aware device scheduling for federated learning at the wireless edge," *IEEE Trans. Wireless Commun.*, vol. 20, no. 6, pp. 3643–3658, 2021.
- [16] B. Luo, X. Li, S. Wang, J. Huang, and L. Tassiulas, "Cost-effective federated learning in mobile edge networks," *IEEE J. Sel. Areas Commun.*, vol. 39, no. 12, pp. 3606–3621, 2021.
- [17] L. Ye and V. Gupta, "Client scheduling for federated learning over wireless networks: A submodular optimization approach," in *Proc. IEEE CDC*, 2021, pp. 63–68.
- [18] W. Shi, S. Zhou, and Z. Niu, "Device scheduling with fast convergence for wireless federated learning," in *Proc. IEEE ICC*, 2020, pp. 1–6.
- [19] I. Mohammed, S. Tabatabai, A. Al-Fuqaha, F. E. Bouanani, J. Qadir, B. Qolomany, and M. Guizani, "Budgeted online selection of candidate

- IoT clients to participate in federated learning," *IEEE Internet Things J.*, vol. 8, no. 7, pp. 5938–5952, 2021.
- [20] H. H. Yang, Z. Liu, T. Q. S. Quek, and H. V. Poor, "Scheduling policies for federated learning in wireless networks," *IEEE Trans. Commun.*, vol. 68, no. 1, pp. 317–333, 2020.
- [21] J. Zhang, S. Chen, X. Zhou, X. Wang, and Y.-B. Lin, "Joint scheduling of participants, local iterations, and radio resources for fair federated learning over mobile edge networks," *IEEE Trans. Mobile Comput.*, pp. 1–1, 2022.
- [22] A. Taïk, H. Moudoud, and S. Cherkaoui, "Data-quality based scheduling for federated edge learning," in *Proc. IEEE LCN*, 2021, pp. 17–23.
- [23] Y. He, J. Ren, G. Yu, and J. Yuan, "Importance-aware data selection and resource allocation in federated edge learning system," *IEEE Trans. Veh. Technol.*, vol. 69, no. 11, pp. 13 593–13 605, 2020.
- [24] J. Leng, Z. Lin, M. Ding, P. Wang, D. Smith, and B. Vucetic, "Client scheduling in wireless federated learning based on channel and learning qualities," *IEEE Wireless Commun. Lett.*, vol. 11, no. 4, pp. 732–735, 2022.
- [25] L. Liang, H. Ye, and G. Y. Li, "Toward intelligent vehicular networks: A machine learning framework," *IEEE Internet Things J.*, vol. 6, no. 1, pp. 124–135, 2019.
- [26] Q. Zheng, K. Zheng, H. Zhang, and V. C. M. Leung, "Delay-optimal virtualized radio resource scheduling in software-defined vehicular networks via stochastic learning," *IEEE Trans. Veh. Technol.*, vol. 65, no. 10, pp. 7857–7867, 2016.
- [27] Y. Lv, Y. Duan, W. Kang, Z. Li, and F.-Y. Wang, "Traffic flow prediction with big data: A deep learning approach," *IEEE Trans. Intell. Transp. Syst.*, vol. 16, no. 2, pp. 865–873, 2015.
- [28] Z. Du, C. Wu, T. Yoshinaga, K.-L. A. Yau, Y. Ji, and J. Li, "Federated learning for vehicular Internet of Things: Recent advances and open issues," *IEEE Open J. Computer Society*, vol. 1, pp. 45–61, 2020.
- [29] D. Jallepalli, N. C. Ravikumar, P. V. Badarinarath, S. Uchil, and M. A. Suresh, "Federated learning for object detection in autonomous vehicles," in *Proc. IEEE BigDataService*, 2021, pp. 107–114.
- [30] J. Posner, L. Tseng, M. Aloqaily, and Y. Jararweh, "Federated learning in vehicular networks: Opportunities and solutions," *IEEE Network*, vol. 35, no. 2, pp. 152–159, 2021.
- [31] S. Liu, J. Yu, X. Deng, and S. Wan, "FedCPF: An efficient-communication federated learning approach for vehicular edge computing in 6G communication networks," *IEEE Trans. Intell. Transp. Syst.*, vol. 23, no. 2, pp. 1616–1629, 2022.
- [32] X. Huang, P. Li, R. Yu, Y. Wu, K. Xie, and S. Xie, "Fedparking: A federated learning based parking space estimation with parked vehicle assisted edge computing," *IEEE Trans. Veh. Technol.*, vol. 70, no. 9, pp. 9355–9368, 2021.
- [33] F. Tang, B. Mao, N. Kato, and G. Gui, "Comprehensive survey on machine learning in vehicular network: Technology, applications and challenges," *IEEE Commun. Surveys Tuts.*, vol. 23, no. 3, pp. 2027–2057, 2021.
- [34] A. M. Elbir, B. Soner, S. Çöleri, D. Gündüz, and M. Bennis, "Federated learning in vehicular networks," in *Proc. IEEE MeditCom*, 2022, pp. 72–77.
- [35] D. Ye, R. Yu, M. Pan, and Z. Han, "Federated learning in vehicular edge computing: A selective model aggregation approach," *IEEE Access*, vol. 8, pp. 23 920–23 935, 2020.
- [36] Z. Yu, J. Hu, G. Min, H. Xu, and J. Mills, "Proactive content caching for Internet-of-Vehicles based on peer-to-peer federated learning," in *Proc. IEEE ICPADS*, 2020, pp. 601–608.
- [37] X. Zhou, W. Liang, J. She, Z. Yan, and K. I.-K. Wang, "Two-layer federated learning with heterogeneous model aggregation for 6G supported internet of vehicles," *IEEE Trans. Veh. Technol.*, vol. 70, no. 6, pp. 5308–5317, 2021.
- [38] P. K. Sangdeh, C. Li, H. Pirayesh, S. Zhang, H. Zeng, and Y. T. Hou, "CF4FL: A communication framework for federated learning in transportation systems," *IEEE Trans. Wireless Commun.*, vol. 22, no. 6, pp. 3821–3836, 2023.
- [39] H. Xiao, J. Zhao, Q. Pei, J. Feng, L. Liu, and W. Shi, "Vehicle selection and resource optimization for federated learning in vehicular edge computing," *IEEE Trans. Intell. Transp. Syst.*, vol. 23, no. 8, pp. 11 073–11 087, 2022.
- [40] M. F. Pervej, R. Jin, and H. Dai, "Resource constrained vehicular edge federated learning with highly mobile connected vehicles," *IEEE J. Sel. Areas Commun.*, vol. 41, no. 6, pp. 1825–1844, 2023.
- [41] B. Xie, Y. Sun, S. Zhou, Z. Niu, Y. Xu, J. Chen, and D. Gunduz, "MOB-FL: Mobility-aware federated learning for intelligent connected vehicles," in *Proc. IEEE ICC*, 2023, pp. 3951–3957.
- [42] Q. Wu, X. Wang, Q. Fan, P. Fan, C. Zhang, and Z. Li, "High stable and accurate vehicle selection scheme based on federated edge learning in vehicular networks," *China Commun.*, vol. 20, no. 3, pp. 1–17, 2023.
- [43] G. Wang, F. Xu, H. Zhang, and C. Zhao, "Joint resource management for mobility supported federated learning in internet of vehicles," *Future Gener. Comput. Syst.*, vol. 129, pp. 199–211, 2022.
- [44] H. Abou-zeid, H. S. Hassanein, and S. Valentin, "Optimal predictive resource allocation: Exploiting mobility patterns and radio maps," in *Proc. IEEE Global Commun. Conf.*, 2013, pp. 4877–4882.
- [45] A. C. S. Rodriguez, N. Haider, Y. He, and E. Dutkiewicz, "Network optimisation in 5G networks: A radio environment map approach," *IEEE Trans. Veh. Technol.*, vol. 69, no. 10, pp. 12 043–12 057, 2020.
- [46] M. Hoffmann, P. Kryszkiewicz, and A. Kliks, "Increasing energy efficiency of massive-MIMO network via base stations switching using reinforcement learning and radio environment maps," *Computer Commun.*, vol. 169, pp. 232–242, 2021.
- [47] W. B. Chikha, M. Masson, Z. Altman, and S. B. Jemaa, "Radio environment map based inter-cell interference coordination for massive-MIMO systems," *IEEE Trans. Mobile Comput.*, 2022.
- [48] M. Hoffmann and P. Kryszkiewicz, "Beam management driven by radio environment maps in O-RAN architecture," *arXiv e-prints*, p. arXiv:2303.11742, 2023.
- [49] —, "Radio environment map and deep Q-learning for 5G dynamic point blanking," in *Proc. SoftCOM*, 2022, pp. 1–3.
- [50] X. Li, K. Huang, W. Yang, S. Wang, and Z. Zhang, "On the convergence of FedAvg on non-IID data," in *Proc. ICLR*, 2019.
- [51] K. Xiong, S. Leng, C. Huang, C. Yuen, and Y. L. Guan, "Intelligent task offloading for heterogeneous V2X communications," *IEEE Trans. Intell. Transp. Syst.*, vol. 22, no. 4, pp. 2226–2238, 2021.
- [52] K. Sato and T. Fujii, "Kriging-based interference power constraint: Integrated design of the radio environment map and transmission power," *IEEE Trans. Cogn. Commun. Netw.*, vol. 3, no. 1, pp. 13–25, 2017.
- [53] K. Sato, K. Suto, K. Inage, K. Adachi, and T. Fujii, "Space-frequency-interpolated radio map," *IEEE Trans. Veh. Technol.*, vol. 70, no. 1, pp. 714–725, 2021.
- [54] V.-P. Chowdappa, C. Botella, J. J. Samper-Zapater, and R. J. Martinez, "Distributed radio map reconstruction for 5G automotive," *IEEE Intell. Transp. Syst. Mag.*, vol. 10, no. 2, pp. 36–49, 2018.
- [55] L.-C. Chen, G. Papandreou, F. Schroff, and H. Adam, "Rethinking atrous convolution for semantic image segmentation," *arXiv e-prints*, p. arXiv:1706.05587, 2017.
- [56] A. Howard, M. Sandler, G. Chu, L.-C. Chen, B. Chen, M. Tan, W. Wang, Y. Zhu, R. Pang, V. Vasudevan *et al.*, "Searching for mobilenetv3," in *Proc. IEEE/CVF ICCV*, 2019, pp. 1314–1324.
- [57] OSM. (2023) *OpenStreetMap*. Accessed on: Nov. 15, 2023. [Online]. Available: <https://www.openstreetmap.org/#map=6/42.088/12.564>
- [58] Mathworks. (2023) *5G Toolbox*. Accessed on: Nov. 15, 2023. [Online]. Available: https://www.mathworks.com/help/5g/index.html?s_tid=CRUX_lftnav
- [59] 3GPP, "Study 3D Channel Model for LTE," 3rd Generation Partnership Project (3GPP), Technical Specification (TS) 36.873, 01 2018, version 12.7.0.
- [60] ITU-R, "Guidelines for Evaluation of Radio Interface Technologies for IMT-Advanced," Technical Report M.2135, 2008.
- [61] 3GPP, "NR; Physical channels and modulation," 3rd Generation Partnership Project (3GPP), Technical Specification (TS) 38.211, 2020.
- [62] —, "NR; Multiplexing and channel coding," 3rd Generation Partnership Project (3GPP), Technical Specification (TS) 38.212, 2020.
- [63] —, "NR; Physical layer procedures for data," 3rd Generation Partnership Project (3GPP), Technical Specification (TS) 38.214, 2020.
- [64] N. Dal Fabbro, S. Dey, M. Rossi, and L. Schenato, "SHED: A Newton-type algorithm for federated learning based on incremental Hessian eigenvector sharing," *arXiv e-prints*, p. arXiv:2202.05800, 2022.